Spatiotemporal Wind Energy Assessment for Transmission Network Integration Considering the Location of Electrical Substations and Loads

Kwabena A. Kyeremeh, Rosemary E. Alden, Aron Patrick[1], and Dan M. Ionel

SPARK Laboratory, Stanley and Karen Pigman College of Engineering, University of Kentucky, Lexington, KY, USA
[1]PPL Corporation, Allentown, PA, USA

kwabena.kyeremeh@uky.edu, rosemary.alden@uky.edu, alpatrick@pplweb.com, dan.ionel@ieee.org

***Abstract*—Wind energy is an abundant renewable resource that can support decarbonization of energy supply. It is, therefore, essential to conduct a comprehensive assessment of wind energy potential for effective transmission network planning and integration. This work introduces a spatial-temporal assessment methodology for wind energy name plate-rated power capacity that considers the locations of electrical substations and transmission lines. This methodology applies Geographic Information System (GIS) land cover data to define siting exclusions for wind turbine installations. The correlation between generated wind power and estimates of power system load, as well as capacity factor, on a sub-regional basis for specific latest generation low and very low wind speed turbines, is estimated. A case study for the proposed methodology is conducted for the Commonwealth of Kentucky, USA with state-of-the-art wind turbines, land cover data from the National Land Cover Database (NLCD), and publicly available spatiotemporal wind data from the NASA EarthData Pathfinder dataset. The results indicate the availability of suitable land for wind turbine deployment, which can contribute to fulfilling the regional annual energy requirement, even with the example restricted sitting exclusion scenario in which turbines must be within 10km distance of a substation.**

***Index Terms*—wind energy, GIS, spatiotemporal variability, load matching, substation, transmission network**

I. Introduction

Wind energy has emerged as an integral component in the global generation mix, offering a promising solution to reduce greenhouse emissions [1–3]. According to the 2024 Global Wind Report, new wind power installations in 2023 reached approximately 117GW, including 10.8GW offshore and 106GW onshore developments [4]. With the rapid growth of the wind energy industry, an accurate and comprehensive assessment of its potential provides scientific insights for policymakers to identify suitable sites for wind farm projects. Spatiotemporal wind energy potential assessment considers both spatial and temporal variations in wind characteristics.

Recent studies have focused on the relevance of advanced methodologies, including machine learning, spatial optimization, and spatiotemporal analysis, to accurately estimate wind energy potential across regions [5, 6]. Siyal *et al.* assessed the wind energy potential available in Sweden using a GIS-based approach [7]. Within the reference, the technical potential for onshore wind energy is estimated by considering system performance, topographic limitations, environmental factors, and land use constraints. The results show that Sweden has sufficient wind energy and enough land area for developing wind farm projects.

The authors in [8] analyzed the impact of land use and turbine technology on wind energy potential. Among the three siting regimes studied, exclusions related to infrastructure setbacks were found to have the greatest impact on wind energy potential. The main influencing factors on captured energy include larger rotor diameters and increased turbine tip heights for greater wind speed per location, even with associated infrastructural setbacks from transporting very large components. Similar work was undertaken in [9] and further extended to quantify the cost of intermittency of wind power.

The complementarity between solar PV and wind energy resources may be utilized to enhance DER generation and integration to meet the demand in a region [10]. Jain *et al.* utilized geospatial and multi-year hourly meteorological datasets to estimate geographical and techno-economic renewable energy potential [11]. It was found that solar and wind had complementary relations in the example region and thus demonstrated the feasibility of hybrid generation to ensure a reliable source of green energy.

This work extends the study from the same research group, which developed an approach to assess the spatiotemporal capacity potential of DERs with applied EOFs and max-p unsupervised learning techniques to identify zones of similar output power [12]. This continued study adds further contributions through wind farm site exclusions based on transmission line and electrical substation proximity in an effort to fill a gap in the academic literature for wind energy potential assessment methods that consider both natural resources and existing infrastructure. Capacity factor on a sub-regional basis, defined by coordinate grid cells, for specific latest generation low and very low wind speed turbines, is estimated in this work. Estimates for the correlation between wind power and power system loads, which indicates the necessity for energy storage systems, are also provided.

The contents are organized as follows: data processing and the proposed assessment methodology in the second section, while the third section describes the example regional spa-

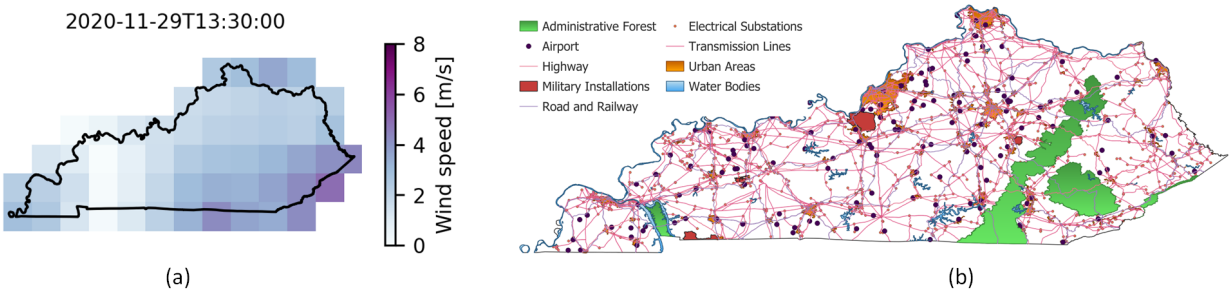

Fig. 1. Spatial distribution of wind speed at 50m for the example region of Kentucky, at a selected time of day (a), obtained from the open source NASA EarthData Pathfinder dataset. Land cover types and facilities excluded from the land cover data (b), in determining suitable land for wind turbine deployment.

tiotemporal case study from public, freely available sources. In the sequence, the fourth section analyzes the results, and the final section summarizes the most important conclusions, contributions, and proposals for further research.

II. Data Processing and Assessment Techniques

Hourly wind data with a spatial resolution of 50km by 50km at an altitude of 50m shown in Fig. 1(a), was obtained from the open source NASA Earthdata Pathfinder MERRA-2 reanalysis climate dataset [13]. The data is extrapolated to determine wind speed at hub height of a turbine as described in [14]:

$$U_{Z_{hub}}(t,x,y) = U_{Z_r}(t,x,y)\left(\frac{Z_{hub}}{Z_r}\right)^{\alpha}, \tag{1}$$

where $U_{Z_{hub}}$ is the wind velocity at turbine hub height, Z_{hub}, and U_{Z_r} the velocity at the reference measurement height, i.e. 50m in this case. The friction coefficient, α, is set to the land cover type of the maximum area within a grid cell.

Availability of land for wind farm deployment, which depends on land use type, plays a crucial role in harnessing wind power [15]. To determine suitable locations, the study excluded specific land cover types and facilities, all of which are detailed in 1(b). Data from the National Land Cover Database [16], with classifications for each 30m by 30m grid cell, was utilized as illustrated in Fig. 2(a). Land cover types and facilities such as bodies of water, roads, highways, railways, protected forests, airports, urban areas, transmission lines, and electrical substations were excluded, together with a buffer zone sized for safety and industry practices.

The site exclusions also included military facilities, mountainous, and high-elevated areas without buffer zones because these areas were assumed not have narrow winding shape, unaccounted for privacy needs, or electrical safety concerns. It is essential to consider the spacing of wind turbine arrays when determining the number of turbines to be deployed on available lands. The layout becomes relevant in decreasing the wake effect, which may reduce energy output and increase the material fatigue for turbines sited downstream [14]. In this study, turbine spacing rules described in [17] were employed.

The wind turbine output power varies by wind speed at hub height, and therefore, manufacturers present a power-speed curve for individual turbines, as illustrated in Fig. 3, to show this variation and represent the effectiveness of their turbines. A power-speed curve was applied in this work to approximate the annual wind energy production of constituent turbines within a wind farm by grid cell with latitude x and longitude y as:

$$E_{actual}(x,y) = \int_0^T P_w(U_{x,y}(t))\,dt, \tag{2}$$

where $E_{actual}(x,y)$ is the energy production of a single turbine in a grid cell, T the period, and $P_w(U_{x,y}(t))$ the turbine output power as a function of time-varying wind speed, according to the turbine power-speed curve. Following the expected variety in output power, the actual energy generated is a fraction of the maximum possible energy output, which is defined as the capacity factor [17] and was calculated as follows:

$$CF(x,y) = \frac{E_{actual}(x,y)}{P_R \times 8760}, \tag{3}$$

where $CF(x,y)$ is the capacity factor of a grid cell, E_{actual} the actual energy delivered in the considered grid cell, and P_R the turbine's rated power.

The correlation between wind power generation and electric network loading indicates the requirement of an energy storage system [18]. The Pearson correlation coefficient was employed in this work to quantify load matching, i.e. the capacity of wind energy generation to meet demand, and was calculated as follows:

$$A = T\sum_{t=1}^{T}(P_{wt}P_{Lt}) - \left(\sum_{t=1}^{T}P_{wt}\right)\left(\sum_{t=1}^{T}P_{Lt}\right), \tag{4}$$

$$B = \left[T\sum_{t=1}^{T}P_{wt}^2 - \left(\sum_{t=1}^{T}P_{wt}\right)^2\right]\left[T\sum_{t=1}^{T}P_{Lt}^2 - \left(\sum_{t=1}^{T}P_{Lt}\right)^2\right], \tag{5}$$

$$LM = \frac{A}{\sqrt{B}}, \tag{6}$$

where LM is the load matching metric, T the timespan, P_w the generated wind power, and P_L the demand.

The wind speed scaling, land coverage exclusions, spatial turbine output power and energy, capacity factor, and load matching metric calculations form a procedure for detailed

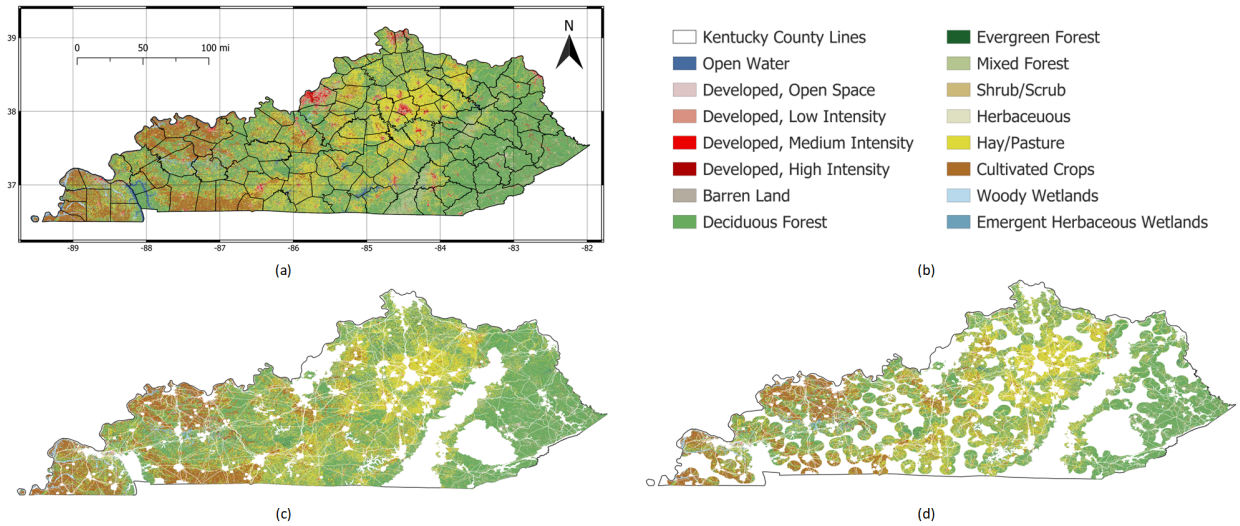

Fig. 2. Land cover data for the Commonwealth of Kentucky (a), with the legend of the land cover types (b). The friction coefficient, utilized in extrapolating wind speed to hub height, is related to land cover type. Maps illustrating the application of relaxed (a) and restricted (b) wind turbine siting exclusions to the study region. Available land after applying the relaxed exclusions is about 77×10^3 km^2 and 59×10^3 km^2 for restricted exclusions, which are approximately 73% and 55%, respectively, of the regional total land area.

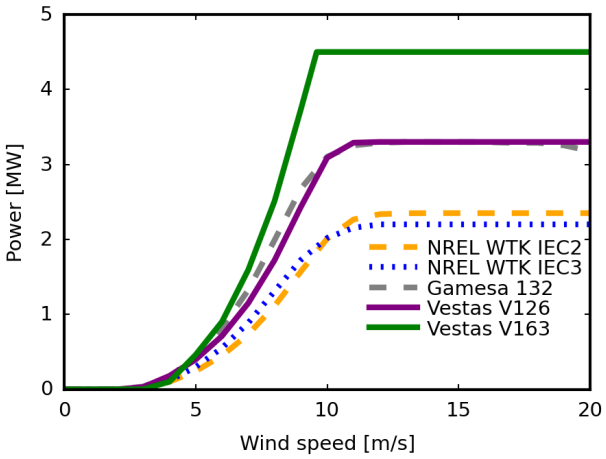

Fig. 3. Power speed curves of example wind turbines of varying wind speed classes by different manufacturers, showing fluctuations in power output due to changes in wind speed.

wind power potential assessment based on public, freely available data. Following wind potential estimates, energy storage sizing for a region may be approximated based on annual imbalances. Specifically, the deficit in supply and excess wind energy generation for the considered region, were also analyzed in this study and calculated as:

$$P_{IM} = \begin{cases} \text{deficit} & \text{if } P_L - P_w < 0 \\ \text{excess} & \text{if } P_L - P_w > 0, \end{cases} \tag{7}$$

where P_{IM} is the power imbalance, P_L the demand, and P_w the generated wind power.

Table I
SUMMARY OF TURBINE SITING EXCLUSIONS AND BUFFER ZONE LIMITS

Exclusion Description	Buffer Zone [m]	Scenarios Relaxed	Scenarios Restricted
National roads, railways, and highways	300	✓	✓
Water bodies	300	✓	✓
Urban areas	1000	✓	✓
Transmission lines and substations	200	✓	✓
Airports	2500	✓	✓
Military installations	-	✓	✓
Administrative forests	1000	✓	✓
Slope $>$ 25%	-	✗	✓
Mountainous areas	-	✗	✓
Proximity to substations and transmission lines	-	✗	✓
Elevation $>$ 1000m	-	✗	✓

III. CASE STUDY: ASSESSING WIND ENERGY POTENTIAL IN KENTUCKY, USA

In this section, the proposed method is applied to the Commonwealth of Kentucky in two subcases of different siting exclusion considerations, including relaxed and restricted scenarios. The relaxed exclusion applies buffer zones to bodies of water, urban areas, airports, national roads, railways, highways, administrative forests, electrical substations, and transmission lines.

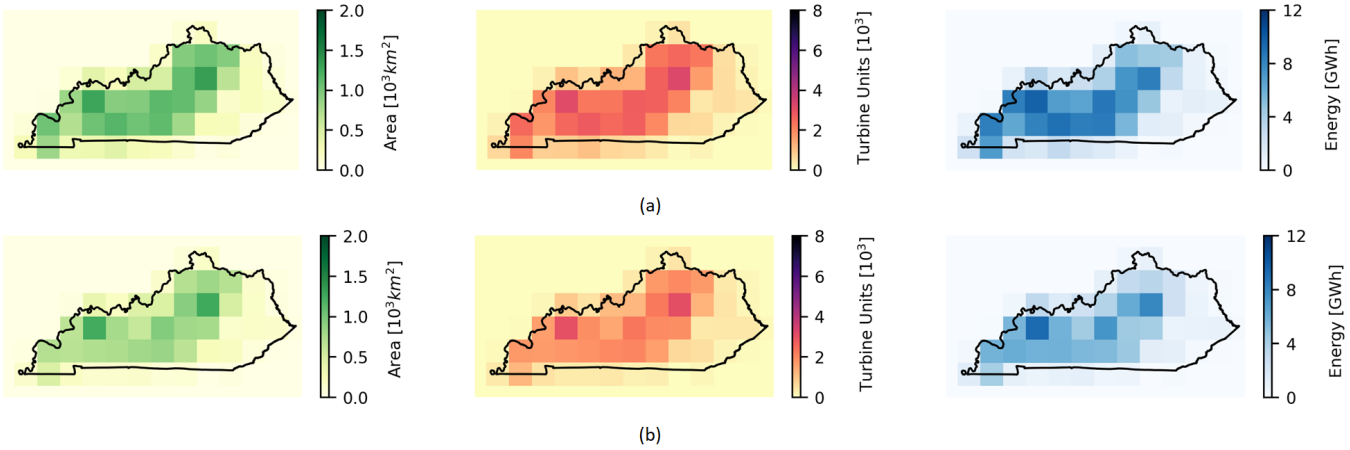

Fig. 4. Available land for wind turbine deployment based on relaxed (a) and restricted (b) turbine siting exclusions for the example land region of Kentucky. The relaxed scenario shows significant land availability and increased turbine deployment, leading to higher energy output in contrast to the restricted case, which highlights the limitations imposed on land use.

Table II
SUMMARIZED RESULTS OF WIND ENERGY POTENTIAL ASSESSMENT OF KENTUCKY UNDER TWO TURBINE SITING EXCLUSIONS

Exclusion Scenario	Available Land [km^2]	Kentucky Land [%]	Turbine Count [unit]	Power Capacity [GW]	Annual Energy [GWh]
Relaxed	76.90×10^3	73	22×10^3	99	186
Restricted	58.95×10^3	55	17×10^3	76.5	138

In addition to the relaxed exclusions, further limitations are applied to form a restricted scenario, which includes mountainous areas, slope above 25%, and a requirement that turbines must be within 10km of an electrical substation. A summary of the exclusions with the applied buffer zones for the considered scenarios is presented in Table I. The available land after each exclusion scenario is shown in Figs. 2(c) and 2(d). Under the relaxed scenario, around 73% of Kentucky's total land is available, while 55% remains available in the restricted scenario.

Within this example case, the 4MW Vestas V163 turbine, designed for low wind speeds according to IEC standards, was selected with a hub height of 140m. In this study, the area required by a turbine is estimated based on a rectangular array of 3 rotor diameters within a row and 5 diameters between rows [17]. As per the criteria detailed in [19], barren land, shrub/scrub, herbaceous, hay/pasture, and cultivated crops are chosen as suitable land cover types for onshore wind deployment. The available land and the total number of deployable wind turbines for the relaxed and restricted exclusion scenarios are visualized in Fig. 4(a) and (b), respectively. Also shown in Fig. 4 is the annual energy output for the example V163 turbine under both siting scenarios. Results for the subcases are summarized in Table II including, available land, turbine count, turbine unit count, power capacity, and annual wind energy generation.

Power imbalance and correlation between wind turbine generation and electrical loads for the considered region is illustrated in Fig. 5. For use with the described procedure,

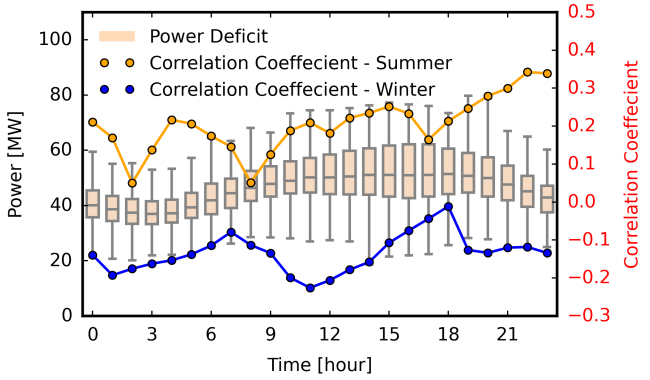

Fig. 5. Seasonal correlation between wind power generation and electrical load within the grid cell with the maximum generation. The variability and range of power deficits, depicting magnitudes and instances of supply imbalances, are also shown.

publicly available aggregated hourly demand data obtained from the U.S. Energy Information Administration [20] was disaggregated based on the population density of each defined grid cell. The hourly power deficit, which is the difference between generated power and system load, identifies peak imbalances and critical periods of the day needing grid stability management by system operators. Correlation coefficient across seasons, reveals important insights into how wind energy generation can effectively match the variation in demand throughout the year. Alternate sources like energy storage systems can be employed by utilities to store or deliver energy during mismatch periods.

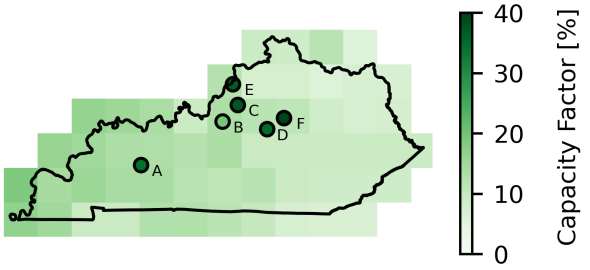

Fig. 6. Capacity factor for the Vestas V163 (IEC IIIb) turbine across defined grid cells in the example region of Kentucky, US, illustrating regional variations in wind energy potential. Point-specific capacity factors, derived from weather stations (A, B, C, D, E, and F) located in the study area, is also shown.

For the example region, a moderate correlation was found for both seasons and across the day, the strongest occurring at night times during the summer. Night-time wind generation at this location serves to complement solar PV output that is most available during the day to meet load imbalances or charge energy storage systems after high imbalances in the evening.

The spatial distribution of capacity factors across grid cells, derived from low spatial and temporal resolution average wind speeds, are illustrated in Fig. 6. The apparent estimates obtained are generally low, demonstrating the limitations of utilizing low-resolution data. Site-specific capacity factors, also shown in Fig. 6, estimated with high-resolution data collected from six weather stations [21], present significantly higher values - ranging from about 20% to 40%.

IV. Discussion

The complementarity between wind energy and solar PV, creates a more reliable renewable energy portfolio that can effectively support grid decarbonization [22, 23]. An estimation of wind energy generation capability may motivate legislation and utilities to consider the technology in their service areas [24, 25]. Spatiotemporal wind energy assessment has a very important role in the initial definition of viable sites for wind turbine installations.

The potential for wind energy generation is inherently represented by the combination of weather resources, i.e. high and low wind speeds, and the availability of wind turbine technology. Recent developments of large rotor diameter and high tip height turbines [26–29], significantly enhance efficient energy generation in low and very low wind speed areas. These technological advancements have increased wind energy generation potential across regions previously considered unsuitable for such installations.

In applying the proposed method in this paper to other regions, turbines have to be definitely selected based on international wind classification standards [30] that correspond to the region's wind speed class. The Delta Wind project [31], with about 40 Vestas V150 low wind speed turbines, sited in Mississippi - a low wind speed region, exemplifies recent expansion of wind energy developments.

To support wind energy integration, a robust power system grid, with sufficient transmission capacity, is important [32]. The proximity of prospective sites to existing electrical substations and transmission lines, and the capacity to host increased generation and demand have to be incorporated in the assessment framework. In addition to technical considerations, national and local regulations on wind turbine siting, designed to address issues including, land use policies, environmental impact, noise restrictions, flight zones, assess restricted areas, and visual impact, must be adhered to.

V. Conclusion

The proposed spatiotemporal wind energy potential assessment for transmission network integration is based on the application of publicly available data to define specific wind turbine siting exclusions in determining suitable locations. An important criterion is the restriction of turbines to within defined distances from transmission lines and electrical substations. This ensures feasible proximity to existing infrastructure, hence minimizing transmission losses and additional infrastructural costs.

Within the proposed methodology, generated energy and sub-regional capacity factors for specific latest generation low and very low wind speed turbines are estimated, highlighting regional variations in wind energy potential over time. Furthermore, the exemplified correlation between wind power generation and electrical load across seasons provides insights into aligning generation and demand. Such metrics become vital to policymakers, who must make informed decisions on wind power projects based on economic viability and environmental impact. A regional case study in Kentucky, USA of the widely applicable proposed framework, illustrated the availability of suitable land for wind turbine deployment and potential contribution to fulfilling the regional annual energy requirement.

Acknowledgment

The support of PPL Corporation and the University of Kentucky L. Stanley Pigman Chair in Power endowment, and of the Lighthouse Beacon Foundation is gratefully acknowledged. Any findings and conclusions expressed herein are those of the authors and do not necessarily reflect the views of the sponsor organizations.

References

[1] F. Blaabjerg and D. M. Ionel, *Renewable energy devices and systems with simulations in MATLAB® and ANSYS®*. Boca Raton, FL: CRC Press, 2017.

[2] Z. Nizamani, N. Cong, M. Khan, A. Nakayama, M. Wahab, K. Fakhruddin, and M. Ahmed, "Performance evaluation of offshore wind turbine support structures - a review," in *2023 12th International Conference on Renewable Energy Research and Applications (ICRERA)*, 2023, pp. 198–202.

[3] F. Ayadi, I. Colak, I. Garip, and H. I. BulBul, "Targets of countries in renewable energy," in *2020 9th International Conference on Renewable Energy Research and Application (ICRERA)*, 2020, pp. 394–398.

[4] Global Wind Energy Council, "Global wind energy report 2024," 2024. [Online]. Available: https://https://gwec.net/global-wind-report-2024/

[5] D. Harrison-Atlas, G. Maclaurin, and E. Lantz, "Spatially-explicit prediction of capacity density advances geographic characterization of wind power technical potential," *Energies*, vol. 14, no. 12, 2021.

[6] Y. Mohd and H. Singh, "Machine learning for analysis and prediction of wind energy," in *2023 International Conference on Circuit Power and Computing Technologies (ICCPCT)*, 2023, pp. 1438–1445.

[7] S. H. Siyal, U. Mörtberg, D. Mentis, M. Welsch, I. Babelon, and M. Howells, "Wind energy assessment considering geographic and environmental restrictions in sweden: A gis-based approach," *Energy*, vol. 83, pp. 447–461, 2015.

[8] A. Lopez, T. Mai, E. Lantz, D. Harrison-Atlas, T. Williams, and G. Maclaurin, "Land use and turbine technology influences on wind potential in the united states," *Energy*, vol. 223, p. 120044, 2021.

[9] Y. Gao, S. Ma, T. Wang, T. Wang, Y. Gong, F. Peng, and A. Tsunekawa, "Assessing the wind energy potential of china in considering its variability/intermittency," *Energy Conversion and Management*, vol. 226, p. 113580, 2020.

[10] A. S. Syed, A. Patrick, A. Lauf, and A. Elmaghraby, "Assessing the complementarity of wind and solar energy in kentucky," *Energies*, vol. 17, no. 13, 2024.

[11] A. Jain, P. Das, S. Yamujala, R. Bhakar, and J. Mathur, "Resource potential and variability assessment of solar and wind energy in india," *Energy*, vol. 211, p. 118993, 2020.

[12] R. E. Alden, C. Halloran, D. D. Lewis, D. M. Ionel, and M. McCulloch, "Assessment of land and renewable energy resource potential for regional power system integration with ml spatio-temporal clustering," in *2023 12th International Conference on Renewable Energy Research and Applications (ICRERA)*, 2023, pp. 618–624.

[13] Global Modeling and Assimilation Office (GMAO), "MERRA-2 tavg1_2d_slv_nx: 2d, 1-Hourly, Time-Averaged, Single-Level,Assimilation, Single-Level Diagnostics V5.12.4," Greenbelt, MD, USA. [Online]. Available: https://disc.gsfc.nasa.gov/datasets/M2T1NXSLV_5.12.4/summary

[14] J. F. Manwell, J. G. McGowan, and A. L. Togers, *Wind Turbine Siting, System Design, and Integration*. John Wiley Sons, Ltd, 2009, ch. 9, pp. 407–448.

[15] M. Hoogwijk, B. de Vries, and W. Turkenburg, "Assessment of the global and regional geographical, technical and economic potential of onshore wind energy," *Energy Economics*, vol. 26, no. 5, pp. 889–919, 2004.

[16] J. Dewitz, "National Land Cover Database (NLCD) 2019 Products," 2021. [Online]. Available: https://www.sciencebase.gov/catalog/item/5f21cef582cef313ed940043

[17] G. M. Master, *Wind Power Systems*. John Wiley Sons, Ltd, 2004, ch. 6, pp. 307–383.

[18] C. Crozier, C. Quarton, N. Mansor, D. Pagnano, and I. Llewellyn, "Modelling of the ability of a mixed renewable generation electricity system with storage to meet consumer demand," *Electricity*, vol. 3, no. 1, pp. 16–32, 2022.

[19] A. Phadke, R. Bharvirkar, and J. Khangura, *Reassessing Wind Potential Estimates for India: Economic and Policy Implications*. Carlifornia: Carlifornia Digital Library. [Online]. Available: https://escholarship.org/content/qt7551z3z3/qt7551z3z3.pdf

[20] U.S. Energy Information Administration, "Electricity grid monitor dashboard: Overview of the u.s.a. electric grid," 2024. [Online]. Available: https://www.eia.gov/electricity/gridmonitor/dashboard/electric_overview/US48/US48

[21] Oklahoma Mesonet, "Mesonet wind data," 2023. [Online]. Available: https://www.mesonet.org/weather/wind

[22] D. D. Lewis, A. Patrick, E. S. Jones, R. E. Alden, A. A. Hadi, M. D. McCulloch, and D. M. Ionel, "Decarbonization analysis for thermal generation and regionally integrated large-scale renewables based on minutely optimal dispatch with a Kentucky case study," *Energies*, vol. 16, no. 4, 2023. [Online]. Available: https://www.mdpi.com/1996-1073/16/4/1999

[23] A. Monterrat, C. Carrejo, S. Hilliard, and F. Devaux, "Integration cost of variable renewable resources to power systems – a techno-economic assessment in european countries," in *2021 10th International Conference on Renewable Energy Research and Application (ICRERA)*, 2021, pp. 210–215.

[24] M. Rambabu, R. S. S Nuvvula, P. P. Kumar, K. Mounich, M. E. Loor-Cevallos, and M. Gupta, "Integrating renewable energy and computer science: Innovations and challenges in a sustainable future," in *2023 12th International Conference on Renewable Energy Research and Applications (ICRERA)*, 2023, pp. 472–479.

[25] A. Harrouz, D. Belatrache, K. Boulal, I. Colak, and K. Kayisli, "Social acceptance of renewable energy dedicated to electric production," in *2020 9th International Conference on Renewable Energy Research and Application (ICRERA)*, 2020, pp. 283–288.

[26] Vestas, "4mw platform brochure," 2024. [Online]. Available: https://nozebra.ipapercms.dk/Vestas/Communication/4mw-platform-brochure/?page=1

[27] S. Gamesa, "Sg 3.4-145 wind turbine," 2024. [Online]. Available: https://www.siemensgamesa.com/global/en/home/products-and-services/onshore/wind-turbine-sg-3-4-145.html

[28] A. Eberle, T. Mai, O. Roberts, T. Williams, P. Pinchuk, A. Lopez, M. Mowers, J. Mowers, T. Stehly, and E. Lantz, "Incorporating wind turbine choice in high-resolution geospatial supply curve and capacity expansion models," National Renewable Energy Laboratory, Golden, CO, Tech. Rep. NREL/TP-6A20-87161, 2024.

[29] F. Author and F. Coauthor, "A parametric model for wind turbine power curves incorporating environmental conditions," *Journal of Renewable Energy*, vol. 45, no. 2, pp. 123–134, 2023.

[30] *IEC 61400-1: Wind Turbines - Part 1: Design Requirements*, International Electrotechnical Commission (IEC) Std., 2019, wind Speed Classification.

[31] AES Corporation, "Delta wind farm," 2024. [Online]. Available: https://www.aes.com/delta-wind-farm

[32] O. M. Akeyo, A. Patrick, and D. M. Ionel, "Study of renewable energy penetration on a benchmark generation and transmission system," *Energies*, vol. 14, no. 1, 2021.